Journal of Neurochemistry, 2005, **92**, 1265–1276 doi:10.1111/j.1471-4159.2004.03006.x

In vitro and *in vivo* analyses of human embryonic stem cell-derived dopamine neurons

Chang-Hwan Park,*,§ Yang-Ki Minn,* Ji-Yeon Lee,†,§ Dong Ho Choi,¶ Mi-Yoon Chang,†,§ Jae-Won Shim,†,§ Ji-Yun Ko,†,§ Hyun-Chul Koh,‡,§ Min Jeong Kang,‡,§ Jin Sun Kang,*,§ Duck-Joo Rhie,** Yong-Sung Lee,†,§ Hyeon Son,†,§ Shin Yong Moon,†† Kwang-Soo Kim‡‡ and Sang-Hun Lee†,§

*Departments of *Microbiology, †Biochemistry and ‡Pharmacology, College of Medicine, and §Institute of Mental Health, Hanyang University, Seoul, Korea*

¶Department of Surgery, College of Medicine, Soonchunhyang University, Seoul, Korea

***Department of Physiology, College of Medicine, The Catholic University of Korea, Seoul, Korea*

††Department of Obstetrics and Gynecology, IRMP, MRC, College of Medicine, Seoul National University, Seoul, Korea

‡‡Molecular Neurobiology Laboratory; McLean Hospital/Harvard Medical School, Belmont, Massachusetts, USA

Abstract

Human embryonic stem (hES) cells, due to their capacity of multipotency and self-renewal, may serve as a valuable experimental tool for human developmental biology and may provide an unlimited cell source for cell replacement therapy. The purpose of this study was to assess the developmental potential of hES cells to replace the selectively lost midbrain dopamine (DA) neurons in Parkinson's disease. Here, we report the development of an *in vitro* differentiation protocol to derive an enriched population of midbrain DA neurons from hES cells. Neural induction of hES cells co-cultured with stromal cells, followed by expansion of the resulting neural precursor cells, efficiently generated DA neurons with concomitant expression of transcriptional factors related to midbrain DA development, such as Pax2, En1 (Engrailed-1), Nurr1, and Lmx1b. Using our procedure, the majority of differentiated hES cells (> 95%) contained neuronal or neural precursor markers and a high percentage (> 40%) of TuJ1+ neurons was tyrosine hydroxylase (TH)+, while none of them expressed the undifferentiated ES cell marker, Oct 3/4. Furthermore, hES cell-derived DA neurons demonstrated functionality *in vitro,* releasing DA in response to KCl-induced depolarization and reuptake of DA. Finally, transplantation of hES-derived DA neurons into the striatum of hemi-parkinsonian rats failed to result in improvement of their behavioral deficits as determined by amphetamine-induced rotation and step-adjustment. Immunohistochemical analyses of grafted brains revealed that abundant hES-derived cells (human nuclei+ cells) survived in the grafts, but none of them were TH+. Therefore, unlike those from mouse ES cells, hES cell-derived DA neurons either do not survive or their DA phenotype is unstable when grafted into rodent brains.

Keywords: dopamine neurons, human embryonic stem cells, *in vitro* differentiation, Parkinson's disease, transplantation.

J. Neurochem. (2005) **92,** 1265–1276.

Received October 7, 2004; revised manuscript received November 23, 2004; accepted November 29, 2004.

Address correspondence and reprint requests to Sang-Hun Lee, Department of Biochemistry, College of Medicine, Hanyang University, #17 Haengdang-dong, Sungdong-gu, Seoul, 133–791, Korea.
E-mail: leesh@hanyang.ac.kr

Abbreviations used: BDNF, brain-derived neurotrophic factor; bFGF, basic fibroblast growth factor; DA, dopamine; DAT, dopamine transporter; En1, engrailed-1; ES, embryonic stem; FGF8, fibroblast growth factor 8; GDNF, glial-derived neurotrophic factor; GFAP, glial fibrillary acidic protein; hES, human embryonic stem; HN, human nuclei; KSR, Knockout serum replacement; MAP2, Microtubule associated protein 2; NT3, neurotrophin-3; MEF, Mouse embryonic fibroblasts; 6-OHDA, 6-hydroxydopamine; PCNA, Proliferating cell nuclear antigen; PD, Parkinson's disease; SHH, sonic hedgehog; TH, tyrosine hydroxylase; TuJ1, neuron-specific class III beta-tublin.

Cell replacement therapy aims at grafting therapeutically relevant cells to impaired tissues and has been proposed for future therapies of intractable neurodegenerative disorders. Parkinson's disease (PD), characterized by progressive and selective loss of dopamine (DA) neurons in the midbrain substantia nigra, is a prime target for cell replacement therapy, given over a decade of successful clinical experiences with fetal ventral mesencephalic cell transplantation in PD patients (Piccini *et al*. 1999). However, fetal cell transplantation has significant technical, ethical, and practical limitations, partly due to limited availability and variable outcomes (Freed *et al*. 2001). Due to their self-renewal capacity and multi-lineage developmental potential, stem cells could be ideal cell sources for cell replacement therapy.

Embryonic stem (ES) cells, derived from the inner cell mass of pre-implantation embryo, are capable of unlimited cell expansion *in vitro* while maintaining their pluripotency. When exposed to appropriate culture conditions and/or genetic manipulation, ES cells can differentiate into multi-lineage cell types that are clinically relevant. Furthermore, recent progress in establishing somatic cell nuclear transfer ES cells (Hwang *et al*. 2004), referred to as 'therapeutic cloning', raises the possibility of using ES cell-based cell replacement therapy without immune rejection.

Directed differentiation to a specific cell type is the first step towards exploiting the potential of ES cells for cell replacement therapies. Several protocols including embryoid body-based lineage selection (Lee *et al*. 2000a), and co-culture with stromal cells (Kawasaki *et al*. 2000) have been introduced to direct mouse ES cells to differentiate towards midbrain DA neurons. After grafting into the striatum of Parkinsonian rats, mouse ES cell-derived DA neurons survived, integrated into the host striatum and provided functional improvements (Bjorklund *et al*. 2002; Kim *et al*. 2002; Shim *et al*. 2004). While these findings support ES cells usage for cell replacement therapy for the treatment of PD, it is imperative to test the therapeutic potential of human ES (hES) cells. Toward this long-term goal, we here report that midbrain-like DA neurons can be efficiently derived from hES cells. Furthermore, we assessed *in vitro* functionality of hES cell-derived DA neurons and performed their *in vivo* functional assays using experimental Parkinsonian rats grafted with these hES-derived DA cells.

Materials and methods

Culture for maintaining undifferentiated hES cells

Human ES cell lines, HSF-6 (established at University of California, San Francisco, XX, passages 40–60), SNU-hES-3 [Seoul National University (SNU) Hospital, Seoul, Korea, XY, passages 70–85], and Miz-hES-1 (MizMedi Hospital-SNU, Seoul, Korea, XY, passages 35–50) were maintained as described previously (Reubinoff *et al*. 2000; Park *et al*. 2003). Briefly, undifferentiated hES cells were propagated on a feeder layer of γ-irradiated mouse (CF1, Charles River Kingston, Kingston, NY, USA) embryonic fibroblasts (MEF) in ES-medium [DMEM/F12 (Invitrogen, Grand Island, NY, USA) supplemented with 20% (v/v) knockout serum replacements (KSR, Invitrogen, Carlsbad, CA, USA), penicillin (100 IU/mL, Invitrogen) and streptomycin (100 μg/mL, Invitrogen), 0.1 mM nonessential amino acids (Invitrogen), 0.1 mM mercaptoethanol (Sigma-Aldrich, St. Louis, MO, USA), and 4 ng/mL basic fibroblast growth factor (bFGF, R & D Systems, Minneapolis, MN, USA)]. Medium was changed daily. For the maintenance of undifferentiated hES cells, cultures were passaged about once every week by mechanically dissecting and transferring hES colonies onto freshly prepared MEF feeder.

Differentiation of hES cells

Two different protocols were investigated for neural induction of hES cells; one using direct differentiation without feeders (Fig. 1a) and the other consisting of co-culture on a feeder layer of PA6 stromal cells (Kawasaki *et al*. 2000) or PA6 cells stably overexpressing sonic hedgehog (PA6-SHH) (Fig. 2a). PA6 stromal cells were maintained and the stromal feeders were prepared as described previously (Kawasaki *et al*. 2000). The PA6-SHH stable cell line has been established by viral transduction using a retroviral construct expressing human SHH N-terminus (generous gift from Dr Suh-Kim at Ajou University, Korea) followed by blasticidin (5 μg/mL, Invitrogen) selection. Undifferentiated hES colonies were detached from MEF feeders by incubation with 200 U/mL collagenase IV (Invitrogen) for 60 min at 37°C, followed by gentle dissociation into small clusters and then cells were resuspended in serum-free insulin/transferrin/selenium (ITS) medium (Okabe *et al*. 1996) with 0.2 mM ascorbic acid (AA, Sigma-Aldrich). Clusters were plated on intact culture dish surface (for the direct differentiation method) or on a layer of PA6 stromal cell feeder (for the co-culture method). In the direct differentiation protocol without feeder, rosette-like structures were formed by 2–3 weeks of culture in ITS + AA. Only the clusters of rosette structures were mechanically dissected and were grown as floating spheres in N2 (Johe *et al*. 1996) supplemented with bFGF (20 ng/mL) and AA (0.2 mM). After 1 week in culture, intact spheres were transferred onto coverslips (Bellco, Vineland, NJ, USA) precoated with poly L-ornithine (PLO, 15 μg/mL, Sigma-Aldrich)/fibronectin (FN, 1 μg/mL, Sigma-Aldrich) and maintained in N2 for cell differentiation. The other approach consisted of dissociating the spheres into single cells by incubation in Ca^{+2}/Mg^{+2}-free Hank's balanced salt solution (HBSS) for 1 h followed by plating on coated coverslips at 1–2 × 10^5 cells/cm^2 in N2 + bFGF. After an added 4–6 days in culture, cell differentiation was induced by withdrawal of bFGF.

In the co-culture method, cell clusters, cultured for 1 week on the PA6 feeder (stage Ia in Fig. 2a), were passaged on freshly prepared feeder of PA6 or PA6-SHH, and further cultured for 1 week (stage Ib). At the end of the co-culture, clusters of cells were harvested from the stromal feeder, gently triturated by pipeting into clusters of 20–300 cells in N2 + AA supplemented with bFGF and then replated on FN-coated dishes. After 1 week of culture in N2 + AA + bFGF for the expansion of neural precursor cells (stage IIa), cells were transferred in clusters or single cell dissociates on glass coverslips. An additional precursor expansion of 3–4 days in

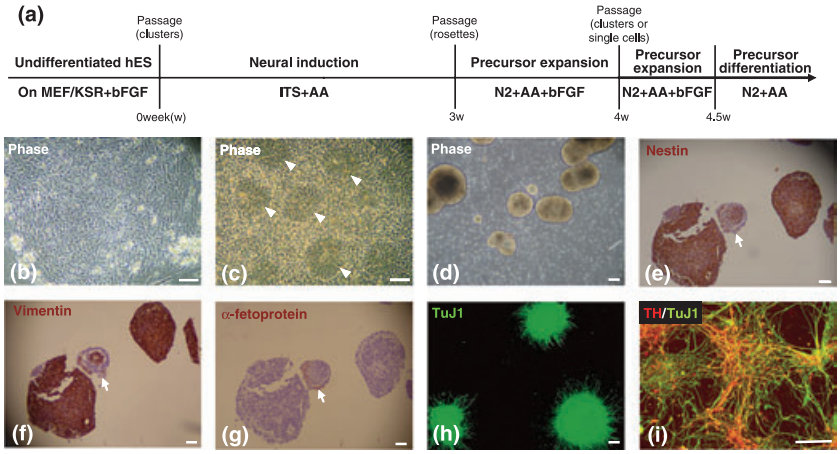

Fig. 1 Neural induction of hES cells by eliminating factors required for maintenance of undifferentiated hES cells. (a) Schematic drawing of the *in vitro* differentiation protocol. (b) A representative colony of undifferentiated hES cell line SNU-hES-3. (c) Neural rosette structures (arrowheads) appear in the center of differentiating cell clusters during neural induction. The clusters of rosette structures were mechanically dissected, and cultured in suspension in the presence of bFGF to form floating cell spheres (d). (e–g) Antigenic properties of the floating spheres. Floating spheres cultured in suspension were embedded in paraffin and sectioned at 4 μm. Images e–g were obtained from neighboring sections. Sections were counter-stained with hematoxylin/eosin. The majority of cells in the spheres stained positive for neural precursor markers nestin (e) and vimentin (f). A small number of cells at the outer layer of a sphere (arrow) were not immunoreactive for these neural precursor markers. (g) Subsets of cells negative for neuronal precursor markers were stained with α-fetoprotein, an endodermal marker (arrow). (h) Acquisition of neuronal marker TuJ1 in hES-derived neurospheres. The spheres in (d) were transferred directly onto FN-coated surface and cultured in absence of bFGF. (i) Representative image of TH/TuJ1-positve neurons derived from hES cell line SNU-hES-3. Human ES-derived spheres in (d) were dissociated into single cells and transferred onto FN-coated dishes. Expansion of single cell isolated precursors was followed by cell differentiation in the absence of bFGF. At day 2 of post bFGF withdrawal, immunofluorescence analyses were carried out. The scale bar is 20 μm.

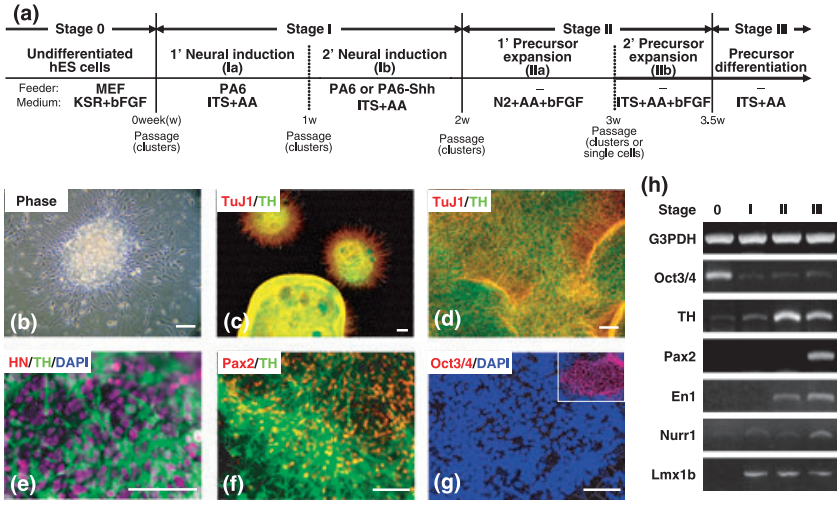

Fig. 2 Stromal feeder-induced derivation of midbrain DA neurons from hES cells. (a) General scheme for the co-culture protocol used for DA differentiation of hES cells. (b) Representative phase-contrast image of differentiated hES colony after neural induction on a layer of PA6 stromal feeder. Human ES cell line HSF-6 was cultured on a layer of PA6 stromal feeder (stage I). After 2 weeks of co-culture, differentiated hES colonies were transferred into FN-coated plates and cultured in the presence of bFGF (stage IIa). The image in (b) was taken 1 day after plating. (c–d) TuJ1/TH+ cell clusters at day 1 (c) and day 7 (d) of stage IIa. (e–g) Antigenic properties of cell clusters differentiated from hES cells were further characterized by immunostaining for HN/TH (e), Pax2/TH (f), and Oct3/4 (g). Inset shows Oct3/4 staining of undifferentiated hES cells at stage 0 as a positive control (g). The scale bar is 20 μm. (h) Expression of genes specific to midbrain development during *in vitro* differentiation of hES cells.

N2 + AA + bFGF (stage IIb), was followed by culture in ITS supplemented with AA (stage III). In certain experiments, cells were treated with cytokines brain-derived neurotrophic factor (BDNF) (20 ng/mL), glial cell-line derived neurotrophic factor (GDNF 20 ng/mL), neurotrophin-3 (NT3) (20 ng/mL), SHH (100–500 ng/mL) and fibroblast growth factor 8 (FGF8; 100 ng/mL), all from R & D Systems, or conditioned medium prepared from neuron-enriched or astrocyte-enriched cultures as previously described (Chang *et al*. 2003).

Immunostaining on cultured cells and brain slices

Floating spheres cultured in suspension were fixed overnight in 10% neutral-buffered formalin, dehydrated in a series of alcohol gradients (70–100%), embedded in paraffin and sectioned at 4 μm. Sections were counter-stained with hematoxylin/eosin. Perfused brain tissues were soaked in 30% sucrose overnight, frozen in Tissue-Tek® (Sakura Finetek USA, Torrance, CA, USA) solution and cut on cryostat at 35 μm. Cultured cells or cryosectioned brain slides were fixed in 4% paraformaldehyde/0.15% picric acid in phosphate buffered saline (PBS) [for γ-aminobutyric acid (GABA) immunostaining, 0.2% glutaraldehyde (Sigma-Aldrich) was included in the fixative]. The following primary antibodies were used: rabbit polyclonal Igs included nestin #130 1 : 50 (Martha Marvin and Ron McKay, National Institute of Heath, Bethesda, MD, USA), tyrosine hydroxylase (TH) 1 : 250 (Pel-Freez, Rogers, AR, USA), and GABA 1 : 700 (Sigma-Aldrich), neuron-specific class III beta-tubulin (TuJ1) 1 : 2000 (Covance, Richmond, CA, USA), Pax 21 : 400 (Covance) and calbindin-D28K 1 : 250 (Chemicon, Temecula, CA, USA). Mouse monoclonal IgG included TH 1 : 1000, CNPase 1 : 500, microtubule associated protein 2 (MAP2) 1 : 200 (Sigma-Aldrich), dopamine β-hydroxylase 1 : 100 (Chemicon), O4 1 : 100 (Chemicon), human nuclei (HN) 1 : 1000 (Chemicon), TuJ1 1 : 500 (Covance), glial fibrillary acidic protein (GFAP) 1 : 100 (ICN Biochem., Aurora, OH, USA), Ki67 1 : 100 (Novocastra, Newcastle, UK), N-CAM 1 : 100, Oct 3/4 (Santa Cruz Biotechnology, Santa Cruz, CA, USA) and proliferating cell nuclear antigen (PCNA) 1 : 40 (Upstate, Charlottesville, VA). Appropriate fluorescence-tagged (Jackson Immunoresearch Laboratories, West Grove, PA, USA) or biotinylated (Vector Laboratories, Burlingame, CA, USA) antibodies were used for visualization. Cells were mounted in VECTASHIELD® containing 4′,6-diamidino-2 phenylindole (DAPI; Vector Laboratories) and analyzed under an epifluorescent microscope (Nikon, Tokyo, Japan).

RT-PCR analysis

Total cellular RNA was isolated using TRI REAGENT (Molecular Research Center, Inc. Cincinnati, OH, USA) and cDNA was synthesized from 5 μg of total RNA in a 20 μL reaction using the Superscript kit (Invitrogen). Optimal PCR conditions for each primer set were determined by varying $MgCl_2$ concentrations and annealing temperatures and cycle numbers to determine linear amplification range. Primer sequences, cycle numbers and annealing temperatures were as follows: G3PDH (5′-GCTCAGACACCATGGGGAAGGT-3′, 5′-GTGGTGCAGGAGGCATTGCTGA-3′, 55°C, 35 cycle, 474 bp); Oct3/4 (5′-CTTGCTGCAGAAGTGGGTGGAGGAA-3′, 5′-CTGCAGTGTGGGTTTCGGGCA-3′, 55°C, 35 cycle, 168 bp); TH (5′-GAGTACACCGCCGAGGAGATTG-3′, 5′-GCGGATATACTGGGTGCACTGG-3′, 62°C, 35 cycle, 279 bp); Nurr1 (5′-TTCTCCTTTAAGCAATCGCCC-3′, 5′-AAGCCTTTGCAGCCCTCACAG-3′, 60°C, 35 cycle, 332 bp); Pax2 (5′-GTACTACGAGACCGGCAGCATC-3′, 5′-CGTTTCCTCTTCTCACCATTGG-3′, 60°C, 35 cycle, 396 bp); Engrailed-1 (En1) (5′-GCAACCCGGCTATCCTACTTATG-3′, 5′-ATGTAGCGGTTTGCCTGGAAC-3′, 60°C, 35 cycle, 247 bp); Lmx1b (5′-ACGAGGAGTGTTTGCAGTGCG-3′, 5′-CCCTCCTTGAGCACGAATTCG-3′, 60°C, 30 cycle, 253 bp).

DA uptake assay

DA uptake assays were conducted according to the methods described previously with modifications (Lee *et al*. 2000b). Cells were washed with PBS and incubated with 50 nM [^{3}H]DA in PBS (51 Ci/mmol, Amersham Co., Buckinghamshire, UK) without or with 10 μM nomifensine (RBI, Natick, MA, USA), a dopamine transporter (DAT) blocker, to determine non-specific uptake. After incubation for 10 min at 37°C, the uptake reactions were terminated by aspiration of the reaction solution and washing twice with ice-cold PBS. Cells were lyzed in 0.5 M NaOH and the radioactivity was measured by liquid scintillation counting (MicroBeta® TriLux ver. 4.4 Wallac, Turku, Finland). Specific DA uptake was calculated by subtracting non-specific uptake (with nomifensine) from uptake value without nomifensine.

Electrophysiology

Cells grown on a coverslip were transferred to the recording chamber and superfused continuously with artificial cerebrospinal fluid (1.5–2 mL/min) containing 125 mM NaCl, 2.5 mM KCl, 2 mM $CaCl_2$, 1 mM $MgSO_4$, 1.25 mM KH_2PO_4, 25 mM $NaHCO_3$, and 25 mM D-glucose, bubbled with 95% O_2/5% CO_2. All recordings were performed at 32–33°C. Standard whole-cell patch-clamp technique with EPC-8 amplifier (Axon Instruments, Union City, CA, USA) was used to record ionic current and membrane potential. The patch electrodes (3–5 MΩ) were filled with a pipette solution containing 130 mM K gluconate, 10 mM KCl, 3 mM MgATP, 10 mM phosphocreatine, 0.3 mM GTP, 10 mM HEPES, 0.2 mM EGTA, 50 U/mL creatine phosphokinase (pH 7.3 with KOH). Whole-cell configuration was obtained after obtaining a tight seal of > 2 GΩ. Membrane current was recorded in voltage-clamp mode with 60% series resistance compensation and membrane potential in current-clamp mode, which was switched during the experiment.

DA determination by HPLC

DA release in the medium conditioned by the differentiated hES cells (stage III of the co-culture method) was determined using reverse phase-HPLC. Differentiated hES cells in 24-well plates were incubated in 200 μL ITS + AA or ITS + AA medium supplemented with 56 mM KCl (evoked) for 30 min. The media were then collected and stabilized with 0.1 mM EDTA and analyzed for DA. Samples (100 μL) were injected with a Rheodyne injector and separated with a reverse phase μ-Bondapak C18 column (150 × 3.0 mm, Eicom, Japan) maintained at 32°C with a column heater (Waters, Cotland, NY, USA). The mobile-phase consisted of 0.05 M citric acid, 0.05 M disodium phosphate (pH 3.1), 3.2 mM 1-octanesulfonic acid (sodium salt), 0.3 mM EDTA and 12%

methanol, and was pumped at a flow rate of 0.5 mL/min using Waters' solvent delivery system (Waters, Milford, MA, USA). Electroactive compounds were analyzed at +650 mV using an analytical cell and an amperometric detector (Eicom, Model ECD-300, Japan). DA levels were calculated using external DA standard injected immediately before and after each experiment.

Transplantation, *in vivo* analysis of grafted cells, and behavioral tests

Animals were housed and treated following National Institutes of Health guidelines. Under phenobarbital anesthesia (50 mg/kg, i.p.), adult male Sprague–Dawley rats (220–250 g) were given unilateral sterotaxic injections of 4 μL of 6-hydroxydopamine (6-OHDA, 3 μg/μL; Sigma-Aldrich) into the substantia nigra [co-ordinates: anteroposterior (AP), −4.8 mm; mediolateral (ML), 1.5 mm; dorsoventral (V), 8.2 mm] and the median forebrain bundle (AP −1.8 mm, ML 1.8 mm, V 8.0 mm). Incisor bar was set at −3.5 mm, AP and ML coordinates are given relative to bregma (Paxinos and Watson, 1982).

For transplantation, differentiated HSF-6 hES cells (day 3 of stage II or III) were harvested and dissociated into single cell suspensions or in cell clusters by incubating in HBSS or collagenase IV, respectively, as described in 'Differentiation of hES cells'. Single cells were resuspended in PBS at a concentration of 10^5 cells/μL. Using a 22-gauge needle, 5 μL of cell suspension was injected over a 5-min period into the ipsilateral striatum (AP +0.2 mm, ML 3.0 mm, V 5.5 mm, incisor bar set at 3.5 mm). The needle was left in place for 3–5 min following the completion of each injection. In other cases, harvested cell clusters were further cultured in ITS + AA + bFGF in ultra low binding culture dishes (Corning, Corning, NY, USA) to form solid floating cell aggregates (diameter: 0.5–1 mm). Eight to 10 of the cell aggregates were injected into the striatum using a 19-gauge spinal needle. Sham-operation was performed on control animals. Rats received daily injections of cyclosporine A (10 mg/kg, i.p.) starting 24 h prior to grafting and continuing for 3 weeks followed by a reduced dose of 5 mg/kg for the remaining *in vivo* period.

Three weeks after 6-OHDA lesioning, animals were tested for rotational asymmetry after i.p. injection of 3 mg/kg D-amphetamine sulfate (Sigma-Aldrich). Animals with an average of ≥ 5 turns/min over a 1 hr interval were selected and randomly assigned to treatment or control groups. Forelimb akinesia was assessed by the 'stepping test' (Olsson *et al*. 1995). Animals were adapted to the test conditions 5 days preceding the actual test. The investigator fixed both hindlimbs as well as one forelimb while the unrestrained forepaw was touching the table. The number of adjusting steps was counted while the rat was moved sideways along the table surface (90 cm in 10 s). Each step test consisted of three trials for each forepaw, alternating between forepaws. In all experiments, the average of three trials for each forepaw was used for analysis. The results were expressed as a percentage of steps performed with the lesioned side as compared with the intact side.

In the estimation of rotation and stepping scores 1 day before cell transplantation, no significant differences in the behavioral tests were observed among the groups assigned randomly. The absolute number of rotation for an hour in each group of animals before transplantation were 360.5 ± 22.1 (sham-operated), 343.3 ± 25.5 (clusters-grafted), and 344.2 ± 19.4 (single cells-grafted). Adjusting steps in each group of animals before transplantation were: intact paw: 18.7 ± 2.1 (sham-operated), 18.3 ± 1.8 (clusters-grafted), and 19.1 ± 1.5 (single cells-grafted); lesioned paw: 1.7 ± 0.2 (sham-operated), 1.3 ± 0.3 (clusters-grafted), and 1.4 ± 0.2 (single cells-grafted). The behavioral tests were performed weekly for 6 weeks after cell transplantation.

Two weeks after transplantation, animals were anesthetized with phenobarbital and perfused transcardially with 4% paraformaldehyde in PBS. Brains were equilibrated with 30% sucrose in PBS and sliced on a freezing microtome (CM 1850, Leica, Wetzlar, Germany). Free-floating brain sections (35 μm thick) were subjected to immunohistochemistry as described above.

Results

Direct neural induction of hES cells in the absence of hES cell maintenance factors

It has been suggested that neural lineage defaults from mouse ES cells in the absence of signals for maintaining self-renewal and undifferentiated properties of these cells (Hitoshi *et al*. 2004). To initiate differentiation, colonies of hES cells (SNU-hES-3, Miz-hES-1 or HSF-6), grown on a feeder layer of MEF, were transferred and cultured in the absence of feeder and bFGF, both of which are necessary for the maintenance of undifferentiated hES cell properties. Data shown in this section were obtained from the hES cell line SNU-hES-3, unless specified otherwise, while similar data were obtained with Miz-hES-1 and HSF-6. Under differentiation conditions, the shape of hES colonies was strikingly changed to multilayered clusters of an increasing number of small, elongated cells in the center surrounded by flattened cells. By 2–3 weeks of culture in ITS medium, rosette-like structures, resembling early neural tube, were formed in the clusters (Fig. 1c). The clusters including rosettes were isolated mechanically under microscopic examination and were grown as free-floating suspension culture of cell aggregates in N2 supplemented with bFGF, a specific mitogen for neural precursor cells, for 5–7 days (Fig. 1d). Immunocytochemical analyses revealed that the majority of cells (> 90% of total cells) in the floating aggregates (spheres) were positive for neural precursor cell markers nestin (Fig. 1e) and vimentin (Fig. 1f). None of the cells were positive for desmin, a mesodermal marker (data not shown). The endodermal markers alpha-fetoprotein (Fig. 1g) and PECAM colocalized in 6.9 and 5.8% of the cells, respectively. The spheres were plated directly on FN-coated coverslips and cultured in N2. Five to 7 days after plating, processes emanating from the spheres had formed prominent fiber bundles. Immunofluorescence analyses revealed that the vast majority of the cells in the outgrowth areas expressed the neuronal marker TuJ1 (Fig. 1h). However, the DA neuronal marker TH colocalized only with a minority (< 10 cells per coverslip) of TuJ1+ cells. To increase the yield of TH/TuJ1+

cells, the floating spheres were dissociated into single cells and then plated on FN-coated dishes and cultured in N2 + bFGF. This protocol was based on our assumption that DA neuron precursors assembled inside of aggregates might require to be exposed to the culture environment for their *in vitro* terminal differentiation towards the DA phenotype. Dissociated cells were proliferated in response to bFGF. After 4 days of cell expansion (at 60–80% cell confluency), bFGF was withdrawn from the culture medium to induce cell differentiation. However, under differentiation conditions cell viability plummeted and we were unable to sustain the cultures for longer than 3 days after bFGF withdrawal. Thus, cultures were fixed and cells phenotyped 2 days after bFGF withdrawal. Cells (28.8 ± 3.8%) were positive for the neuronal marker TuJ1 by immunofluorecence detection (Fig. 1h), and 21.6 ± 3.3% of cells positive for TuJ1 expressed TH (Fig. 1i). The vast majority of cells negative for TuJ1 or TH expressed nestin, an intermediate filament specific to neural precursors (50.3 ± 3.1% of total cells), suggesting insufficient differentiation of neural precursor cells. Cell survival of neural precursors derived from hES is described below.

Efficient derivation of midbrain DA cells from the HSF-6 cell line by coculturing with stromal feeder cells

In the protocol described above, mass production of DA neurons was hampered by the laborious mechanical dissection of rosettes. It has been reported that stromal cells can direct neural induction of mouse ES (Kawasaki *et al*. 2000) as well as primate ES cells (Kawasaki *et al*. 2002). Thus, we cultured hES cells on a layer of PA6 stromal cells (stage I, Fig. 2a). A striking difference in neural induction of hES cells among the cell lines was observed on PA6 stromal feeder. Immunocytochemical analyses at the end of stage I, revealed that 92.3 ± 2.5% of HSF-6 colonies were positive for TuJ1. In these colonies, the majority of cells stained positive for the neural precursor marker nestin. In contrast, only 7.7 ± 1.7% and 7.1 ± 2.4% of colonies acquired expression of the neuronal marker TuJ1 in SNU-hES-3 and Miz-hES-1 cells, respectively.

To eliminate the PA6 feeder cells as well as to obtain an increased yield of cells of neuronal lineages, HSF-6 colonies, harvested 2 weeks after co-culture, were disrupted into small clusters and then plated on FN-coated surfaces in N2 + AA supplemented with bFGF (stage IIa). Cell phenotypes were not largely altered after cell passage. At this stage, the majority of cells were positive for nestin. After 1 week of culture with bFGF, total cell numbers increased by 3–5 folds (estimated by viable cell counting after dissociating the clusters into single cells) suggesting an expansion of neural precursor cells at this stage. The expanded clusters were disrupted into smaller clusters and were passaged again for an additional precursor expansion (stage IIb), followed by precursor differentiation (stage III). Interestingly, cell phenotypes (stage IIb) were not significantly altered by bFGF withdrawal (stage III), when the cultures were maintained as cell clusters (see the result section 'Further differentiation of nestin + clusters derived from hES cells' for a detailed description). Cells in the clusters were uniform with small and elongated cell morphology (Fig. 2b). The vast majority of cells were positive for HN, suggesting an efficient elimination of mouse stromal feeder cells (Fig. 2e). Virtually all of the cell clusters contained TH/TuJ1+ cells (Fig. 2c). Cell clusters grew in size in the presence of bFGF and fused together (Fig. 2d). TH/TuJ1+ cells with neuronal shape constituted a major cell population in cultures (Figs 2c and d). Dopamine β-hydroxylase, a noradrenergic or adrenergic neuronal marker, did not colocalized with TH+ cells, suggesting a DA neuronal identity of TH+ cells (data not shown). None of the cells were positive for Oct3/4, an undifferentiated ES cell marker (Fig. 2g). These findings, collectively, suggest an efficient generation of DA neurons from HSF-6 hES cells.

A subset of cells in the clusters was immunoreactive for Pax2, a transcriptional factor specific to midbrain development (Fig. 2f). Semi-quantitative RT-PCR analyses revealed that expression of the markers characteristic of midbrain DA development, such as *En1*, *Nurr1* and *Lmx1b*, was temporally induced during *in vitro* differentiation of hES cells (Fig. 2h). These findings suggest the midbrain DA nature of TH+ cells derived from hES cells. When passaged in the form of cell clusters, the phenotype of cultures including TH+ cells was not significantly altered after at least three passages (> 3 weeks). Furthermore, cells at stage IIa could be stored at − 80°C and reused by simple freeze/thawing in ITS + AA + bFGF containing 10% dimetylsulfoxide (DMSO) without affecting their potential to differentiate into the DA neuronal fate (data not shown).

SHH and FGF8 effects on midbrain DA differentiation of hES cells

Previous work established SHH and FGF8 as crucial factors in the specification of midbrain DA neurons in explant culture (Ye *et al*. 1998) and for mouse ES cell differentiation in culture (Lee *et al*. 2000a). Cells were exposed to SHH and FGF8 during the last half of the PA6 co-culture period (stage Ib) by transferring cell clusters, co-cultured with PA6 feeders for 1 week (stage Ia), onto freshly prepared feeders consisting of PA6-SHH plus FGF8 cytokine treatment (100 ng/mL) (Fig. 2a). Conditioned medium from confluent cultures of PA6-SHH had a comparable effect as 200–500 ng/mL of SHH in increasing cell number in the cultures for precursors isolated from embryonic day 14 rat cortices, confirming the release of SHH from PA6-SHH (data not shown). Total cell numbers at the end of stage Ib was increased by 2–3 folds in cultures exposed to SHH and FGF8, compared to those unexposed, suggesting survival and/or proliferation effects of these cytokines on differentiating hES cells. The effect of

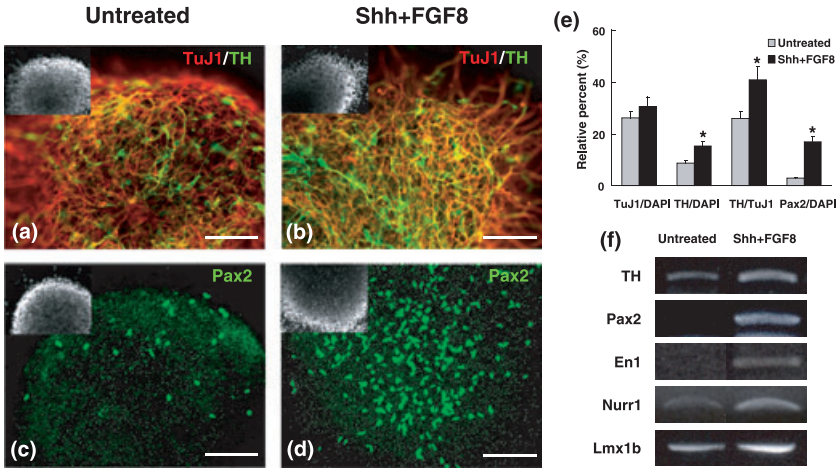

Fig. 3 Effects of SHH and FGF8 on *in vitro* DA derivation from hES cells. For exposure to SHH and FGF8, differentiating hES cells at stage Ia were passaged and cultured on a layer of PA6-SHH in ITS + AA medium supplemented with 100 ng/mL FGF8 (stage Ib). Cells were passaged in the form of cell clusters and the effect of SHH and FGF8 were examined at day 1 of stage IIb. (a and b) Representative images of TH/TuJ1+ clusters of untreated control (a) and cells treated with SHH and FGF8 (b). (c and d) Pax2+ cells in cultures of untreated control (c) and treated with SHH and FGF8 (d). Insets, DAPI nuclear staining of the same field. The scale bar is 20 μm. (e) Percentage of immunoreactive cells. Cells positive for TuJ1 (TuJ1/DAPI), TH (TH/DAPI) and Pax2 (Pax2/DAPI) out of total cells. TH+ cells out of TuJ1+ cells (TH/TuJ1). *Significantly different from control at $p < 0.01$. (f) RT-PCR analysis of genes involved in midbrain DA development. Note that expression of midbrain-specific genes *Pax2*, *En1*, *Nurr1* and *Lmx1b* was enhanced by SHH and FGF8 treatment.

SHH on cell survival/proliferation of neural precursors has been demonstrated previously (Kenney and Rowitch 2000; Lai *et al*. 2003; Machold *et al*. 2003; Thibert *et al*. 2003). The effects of SHH and FGF8 on hES cell differentiation were analyzed at the first day of stage IIb. TuJ1+ neuronal numbers in the cultures pre-exposed to SHH and FGF8 were not significantly different from unexposed control cultures (30.5 ± 3.7 vs. 26.1 ± 1.9% of total cells, $n = 20$, Figs 3a, b and e). However, the percentage of TH+ cells was significantly increased in cultures pre-exposed to SHH and FGF8 (Figs 3a, b and e). Among the TuJ1+ neurons out of total cells, 41.1 ± 3.7% of the cells treated with SHH + FGF8 expressed TH compared to 25.9 ± 3.2% for untreated cells. Another striking effect of SHH and FGF8 treatment was reflected by the percentage of cells positive for Pax2, a specific transcriptional factor of midbrain neuronal development (16.9 ± 3.8 vs. 2.9 ± 1.0% of Pax2+ cells, Figs 3c, d and e). Furthermore, the exposure of SHH and FGF8 led to an enhanced expression of genes specific for midbrain DA neuronal markers such as En1, Nurr1, and Lmx1b as examined by semiquantitative RT-PCR analyses (Fig. 3f). These results suggest a role for SHH and FGF8 on midbrain DA neuronal development during *in vitro* differentiation of hES cells. Subsequent data were obtained with cells co-cultured with PA6-SHH.

Further differentiation of nestin+ clusters derived from hES cells

In addition to TuJ1+ neurons, another major population of cells in the differentiated hES cell clusters consisted of proliferating neural precursors that are positive for both the neural precursor cell marker nestin and the proliferating cell marker Ki67 (nestin/Ki67+ cells, 52.6 ± 3.9% of total cells in stage IIb). The proportion of these cells was not significantly altered by further induction of cell differentiation in the absence of bFGF, suggesting an inadequate differentiation of nestin+ neural precursors assembled in the cell clusters. It has been suggested that clusters of neural precursor cells are proliferating while single isolated precursors take on their differentiation phenotype (Temple and Davis 1994). Thus we assumed that differentiation of neural precursors assembled in the clusters is prevented by cell–cell contacts. For adequate cell differentiation of nestin+ cells, stage IIa clusters were dissociated into single cells, and passaged onto FN-coated coverslips. Passaging cells in the form of cell clusters resulted in excellent cell recovery at stage IIb. In contrast, considerable cell loss was observed in cultures passaged by single cell dissociation: < 30% of the total cells plated were viable after being plated for 1 day. However, surviving cells had high proliferation activity in presence of bFGF reaching 70–90% confluency after 4 days in culture. At this stage, the vast majority of cells (> 95%) expressed nestin (Fig. 4a) but only 3.6 ± 0.1% of the cells were positive for TuJ1, suggesting a selective survival and proliferation of nestin+ precursors in cultures originating from single cell dissociation.

Differentiation of nestin+ precursors was induced by withdrawal of bFGF. Similar to the direct differentiation protocol described above, cells expanded from single cell dissociation exhibited poor viability in N2 or N2 + AA

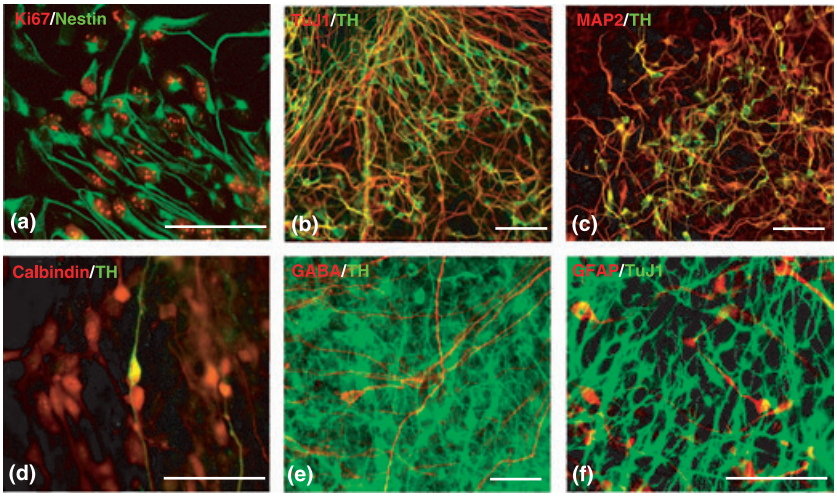

Fig. 4 Further differentiation of hES-derived neural precursor cells. Cell clusters at stage IIa of the co-culture protocol were dissociated into single cells, and plated on FN-coated surface. After 3–4 days of bFGF-expansion, the vast majority of cells expressed nestin (neural precursor cell marker) and the proliferating cell marker Ki67 colocalized with nestin+ cells. (a) Representative image of nestin/Ki67+ cells at day 3 of cell expansion. (b–e) Phenotypes of the cultures differentiated from hES-derived neural precursor cells. Cell differentiation of nestin+ precursors was induced for 7 days in the absence of bFGF. Immunofluorescence analyses were performed for TuJ1/TH (b), MAP2/TH (c), Calbindin/TH (d), GABA/TH (e), and GFAP/TuJ1 (f). The scale bar is 20 μm.

medium without bFGF. Therefore, it was impossible to induce differentiation for more than 2 days. Cell survival was not significantly enhanced by treatment with neurotrophic cytokines (BDNF, GDNF, and NT3) and supplementation with conditioned media from neuron- or astrocyte-enriched cultures. Interestingly, hES-derived precursors cultured in ITS + AA were viable for more than 7 days in the absence of bFGF. After 7 days of differentiation in ITS + AA, 65.6 ± 1.3% of total cells were TuJ1+ neurons, suggesting an efficient differentiation of hES-derived neural precursor cells. Among the TuJ1-positve neuronal population 22.1 ± 1.7% of cells expressed TH (Fig. 4b). The other neuronal markers MAP2 and N-CAM colocalized with TH+ cells (Fig. 4c and data not shown). Less than 0.1% of TH+ cells expressed calbindin, a calcium-binding protein specifically expressed in midbrain DA neurons and which increases resistance to cell death in PD (Yamada *et al*. 1990; Gaspar *et al*. 1994; Damier *et al*. 1999; Fig. 4d). In addition to TH+ neurons, 1.4 ± 0.24% of TuJ1+ neurons were positive for GABA (Fig. 4e). Only a few GFAP+ astrocytes (< 10 cells per coverslip) were detected in the differentiated cultures (Fig. 4f). None of the cells was positive for CNPase and O4, markers for the oligodenrocytic lineage. The number of GFAP+ astrocytes was increased by extension of *in vitro* differentiation, but oligodendrocyte was still not observed after 16 days of differentiation. These findings suggest that nestin+ cells derived from hES cells in the present study may represent neural precursor cells of the early developmental stage, given that neural precursors sequentially yield neuron, astrocytes and oligodendrocytes in the developing brain (Bayer and Altman 1991; Jacobson 1991; Qian *et al*. 2000).

In vitro function of hES-derived TH cells

Cells showing long multiple processes in the peripheral region of stage III cell clusters were chosen for electrophysiological recording ($n = 8$, Fig. 5a). Membrane potential (−22.8 ± 4.3 mV) and whole cell capacitance (86.4 ± 9.5 pF) were measured immediately after membrane perforation. Total membrane current was recorded with the holding potential at −70 mV. All the cells showed fast inward currents and delayed outward currents with slight inactivation (Fig. 5b). Rapidly inactivating A-type currents, which disappeared while holding the potential at −40 mV, was also observed in some cells (5 out of 8 cells). Membrane response to this depolarizing current was recorded in 4 cells under the current-clamp mode. All 4 cells showed generation of action potentials (Fig. 5c). These results showed the presence of well developed sodium and potassium channels, generating action potentials.

An important physiological aspect of authentic DA neuron phenotypes is the ability to synthesize DA and release it in response to membrane depolarization. We measured levels of DA released from hES-derived TH+ cells in the medium conditioned by cultures of stage III HSF-6 cells for 30 min. Without KCl-induced depolarization stimuli, only small amounts of DA were detected in the medium (15.6 ± 3.8 pg/mL of medium, $n = 4$). However, after treatment with 56 mM KCl, the released DA in the media was greatly enhanced (1643 ± 276 pg/mL, $n = 4$), demonstrating depo-

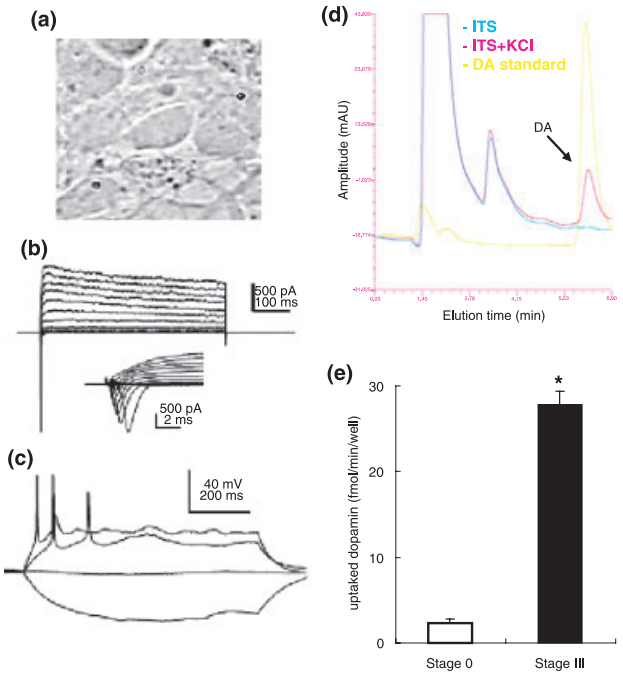

Fig. 5 *In vitro* characterization of differentiated hES cells. (a) Distinct cells located in periphery of neurospheres were chosen for the recordings. (b) Current traces under the voltage-clamp mode. Total membrane currents were measured without any blockers. Step voltage activation (10 mV) from holding at −70 mV evoked inward and outward currents. Inset shows the inward current at the beginning of the step voltage command. (c) Recording of action potentials. Membrane voltage was recorded under the current-clamp mode in the same cell. Action potentials were generated with positive step current injection (10 pA step). (d) HPLC determination of DA levels. Representative HPLC chromatograms for basal DA release (blue line: exposure to ITS + AA medium for 30 min) and DA release after 30 min of KCl-evoked depolarization (red line). The yellow line represents DA standard. (e) DA uptake. The graph depict the specific DA uptake of stage 0 (undifferentiated, white bar, $n = 4$) and stage III (differentiated, black bar, $n = 4$) hES cells. Specific DA uptake was calculated by subtracting non-specific uptake (with nomifensine) from uptake value without nomifensine. *Significantly different from control at $p < 0.01$.

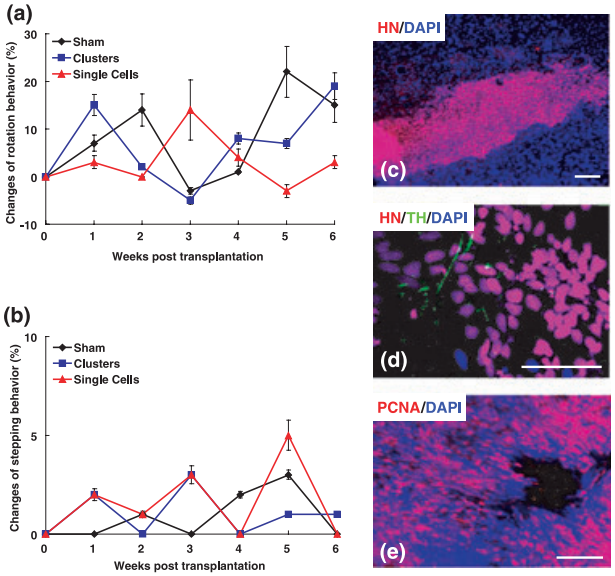

Fig. 6 *In vivo* survival and functions of hES-derived DA neurons. (a and b) Behavioral analysis. Differentiated HSF-6 cells at stage II of the co-culture protocol were harvested and injected in the form of cell clusters ($n = 12$) or single cell dissociates ($n = 8$) into the striatum of hemi-Parkinsonian rats. For negative control, 10 animals were sham-operated under identical schedule as the cell-grafted animals. (a) Amphetamine-induced rotation response. Data are given as mean ± SEM of changes in rotation scores for each animal as compared to pretransplantation values. (b) Stepping test. The results are expressed as a percentage of the lesioned side relative to the number of steps with the non-lesioned paw. (c–e) Immunohistochemical analyses on brain slices of grafted animals. Two weeks after transplantation, grafted animals were killed and immunostaining was performed. Images (c–e) are representatives for HN (c), HN/TH (d), and PCNA (e) staining of rat brains grafted with differentiated hES cell clusters.

larization-induced DA release of hES-derived TH+ neurons (Fig. 5d).

In addition to depolarization-induced release of DA, high affinity reuptake of the transmitter by DAT is a crucial process for presynaptic DA homeostasis. Specific DA uptake was scarcely observed in undifferentiated hES cultures. In contrast, stage III cells displayed avid DA uptake (27.8 ± 1.65 fmol/min/well, $n = 4$, Fig. 5e).

In vivo transplantation of DA neurons derived from hES cells

We investigated if hES-derived DA neurons can elicit *in vivo* function as measured by amelioration of Parkinsonian motor deficits. Differentiated HSF-6 cells (stage II or III) were prepared in the form of single cells or cell aggregates, and were injected into the striatum of hemi-parkinsonian rats. No functional improvement estimated by the amphetamine-induced rotation test (Fig. 6a) and the stepping test (Fig. 6b), was observed in animals grafted with hES-derived DA cells regardless of cell preparation.

In animals grafted with single cell dissociates, histological analysis revealed only a few HN+ cells along the needle tracts (data not shown). In contrast, a striking number of cells were positive for HN in grafts of animals transplanted with cell aggregates (Fig. 6c). Some TH immunoreactivity with unclear neuronal morphology was observed, but none of them colocalized with HN (Fig. 6d). Cells positive for HN (53.3 ± 4.9%) were positive for the proliferating cell marker PCNA (Fig. 6e), raising the possibility of teratoma formation from these proliferative cells. However, Oct3/4+ cells were not seen in any brain slices and no teratomas were observed in animals receiving grafts of hES-derived DA cells. No difference in *in vivo* cell

survival and functions was observed between stage III and stage II cells (data not shown).

Discussion

The efficient derivation of midbrain DA neurons from hES cells is a prerequisite not only for the developmental study of human midbrain DA neurons, but also for realistic cell replacement therapy of PD and novel drug screening. The present study has demonstrated that a highly enriched population of midbrain DA neurons was generated from hES cells. Co-culture of the HSF-6 hES cell line with PA6 stromal cells effectively yielded a high number of DA neurons (up to 41% of TuJ1+ cells), expressing known midbrain DA neuronal markers. Similar to our findings, Zeng *et al*. (2004) reported recently a highly efficient derivation of DA neurons from the BG01 hES cell line, using the same PA6 co-culture method. In contrast to the efficient neural induction of HSF-6 (Fig. 2) and BG01 (Zeng *et al*. 2004) hES cell lines, our study showed that the co-culture method was not effective to direct SNU-hES-3 and Miz-hES-1 cells to differentiate towards neural lineages. The observed difference in their response to the co-culture system may reflect inherent differences of each human embryonic cell line and/or the underlying genetics of the embryos from which the lines were derived. Consistent with this possibility, difference in gene expression patterns among the hES cell lines and the unique gene expression signatures of independently derived hES cell lines have recently been reported (Abeyta *et al*. 2004).

In the present study, we have compared several different *in vitro* differentiation methods including those based on rosette formation, PA6 co-culture, and co-culture with Shh-expressing PA6 cells (PA6-SHH). While we need further investigation to optimize the *in vitro* culture conditions of hES cells, we propose an efficient procedure is as follows (Fig. 2a). Briefly, it consists of neural induction of hES cells on PA6 and PA6-SHH (stage I), bFGF-induced expansion of nestin+ neural precursors (stage II) and terminal differentiation of the nestin+ cells (stage III). Differentiated neurons almost always appeared in the periphery of large cell clusters during *in vitro* differentiation of hES cells, suggesting disruption of close cell–cell contacts inside the cell clusters might be required to facilitate differentiation of hES cells to the neuronal fate. Thus, our protocol consisted of dissociating cell clusters into smaller pieces or all the way to single cells in passage procedures. Similar to our study, Perrier *et al*. (2004) showed recently the efficient hES-derived DA neuronal generation based on co-culture with MS5 and S2 stromal cells. While both approaches gave rise to efficient generation of DA neurons, the conditions in our study allowed for faster (28 days vs. 50 days) and more efficient derivation of neural phenotypes (> 95% of cells were nestin+ precursors or TuJ1+ neurons). However, the proportion of TH/TuJ1+ was higher (60–80%) in the study by Perrier *et al*. (2004) than ours (41%), probably due to the different stromal cells used or the replating method. Notably, our co-culture protocol does not require the mechanical dissection procedure for rosette structures described in the study of Perrier *et al*. (2004), making the *in vitro* mass production of DA neuron more feasible. During neural induction on PA6 stromal cells layer (stage I), two- to threefold increases in total cell number were usually observed. After stage I, hES-derived neural precursor cells could be expanded for 3 weeks without significant loss of DA yield, resulting in about 64-fold increase in total cell number. Numerically, 10–20 TH+ cells are harvested for every undifferentiated hES cells. The other major concern of guided differentiation of ES cells is the efficient elimination of unwanted cells, especially undifferentiated ES cells. None of the cells generated in our procedure was positive for the undifferentiated ES cell marker Oct3/4 at stage IIb and III of hES cultures and in brain sections of animals grafted with differentiated hES cells. Consistent with this, no teratoma was formed in our grafting experiments.

Major functional components of presynaptic DA neurons consist of synthesis of DA neurotransmitter, depolarization-induced release of the transmitter and high affinity reuptake of transmitter by a sodium dependent (DA) transporter (DAT). DAT function is particularly important for regulating DA homeostasis because absence of this transporter could lead to either excess, unregulated dopaminergic transmission or to premature loss of intrasynaptic stores of the transmitter. We demonstrated the presence of electrophysiologically active sodium and potassium channels and generation of action potentials with positive stepped-current injection in hES cell-derived neurons. DA release was evoked by KCl-induced depolarization, suggesting an activity-dependent DA neurotransmission of the hES-derived DA cells. Furthermore we observed a substantial uptake of DA in differentiated hES cell cultures. Taken together, these findings demonstrate that functional DA neurons are efficiently derived from hES cells using our *in vitro* differentiation methods.

The *in vivo* function of hES-derived DA neurons was tested by intrastriatal transplantation into hemi-parkinsonian rats. We did not observe any significant functional improvements in parkinsonian rats grafted with hES-derived DA cells. As none of the postgrafted cells was positive for TH, lack of behavioral recovery in the grafted animal is attributable to the disappearance of DA neurons after grafting. We observed that TH immunoreactivity gradually decreased *in vitro* without significant loss of cell number during the precursor differentiation period (stage III, data not shown), suggesting that hES-derived DA neurons might only temporarily express their dopaminergic properties and thereby be responsible for the loss of TH immunoreactivity after grafting. However, it is also possible that hES-derived DA

neurons selectively undergo apoptotic cell death in the host striatum. Dissimilar to our result of the *in vivo* TH immunostaining, Zeng *et al*. (2004) demonstrated detection of hES-derived cells positive for TH in the rats grafted, even though the number of the TH+ cells was quite few (< 8.8 TH+ cells per 10 brain sections). This discrepancy might be attributable to the differences in the hES cell lines used, cell preparation procedures used for the transplantation (e.g. such as repeated dissociation of cell clusters during the differentiation procedures in our study), and/or the transplantation/immunization protocols. While there is significant discrepancy in TH immunoreactive cells in the grafted animals, both studies demonstrated that survival and behaviors of hES-derived TH+ cells in host striatum after transplantation is quite different from those derived from mouse ES cells (Chung *et al*. 2002; Kim *et al*. 2002; Shim *et al*. 2004) and mesencephalic precursors (Studer *et al*. 1998; Kim *et al*. 2003) which could efficiently integrate, survive, and function to improve motor dysfunctions in rodent models of Parkinson's disease.

Survival and function of donor DA neurons are highly dependent on the host environment; trophic support (Rosenblad *et al*. 1996; Zawada *et al*. 1998) and immunologic factors (Larsson *et al*. 2000). In addition it has been demonstrated that intrinsic factors, in midbrain DA neurons, such as En1 (Simon *et al*. 2001), Nurr1 (Le *et al*. 1999; Perlmann and Wallen-Mackenzie 2004) and Lmx1b (Smidt *et al*. 2000) are crucial for survival and sustained expression of DA properties in midbrain DA cells. Further studies, taking in consideration of these extrinsic and intrinsic factors, should be addressed to achieve *in vivo* survival and function of hES-derived DA neurons.

Acknowledgements

This work was supported by SC-12040 (Stem Cell Research Center of the 21st Century Frontier Research Program) and M1-0104-00-0290 (NRL) funded by the Ministry of Science and Technology, Republic of Korea.

References

Abeyta M. J., Clark A. T., Rodriguez R. T., Bodnar M. S., Pera R. A. and Firpo M. T. (2004) Unique gene expression signatures of independently-derived human embryonic stem cell lines. *Hum. Mol. Genet.* **13**, 601–608.

Bayer S. A. and Altman J. (1991) *Neurocortical Development*. Raven Press, New York.

Bjorklund L. M., Sanchez-Pernaute R., Chung S., Andersson T., Chen I. Y., McNaught K. S., Brownell A. L., Jenkins B. G., Wahlestedt C., Kim K. S. and Isacson O. (2002) Embryonic stem cells develop into functional dopaminergic neurons after transplantation in a Parkinson rat model. *Proc. Natl. Acad. Sci. USA* **99**, 2344–2349.

Chang M. Y., Son H., Lee Y. S. and Lee S. H. (2003) Neurons and astrocytes secrete factors that cause stem cells to differentiate into neurons and astrocytes, respectively. *Mol. Cell. Neurosci.* **2**, 414–426.

Chung S., Sonntag K.-C., Andersson T., Bjorklund L. M., Park J. J., Kim D. W., Kang U. J., Isacson O. and Kim K. S. (2002) Genetic engineering of mouse embryonic stem cells by Nurr1 enhances differentiation and maturation into dopaminergic neurons. *Eur. J. Neurosci.* **16**, 1829–1838.

Damier P., Hirsch E. C., Agid Y. and Graybiel A. M. (1999) The substantia nigra of the human brain. I. Nigrosomes and the nigral matrix, a compartmental organization based on calbindin D (28K) immunohistochemistry. *Brain* **122**, 1421–1436.

Freed C. R., Greene P. E., Breeze R. E., Tsai W. Y., DuMouchel W., Kao R., Dillon S., Winfield H., Culver S., Trojanowski J. Q. *et al.* (2001) Transplantation of embryonic dopamine neurons for severe Parkinson's disease. *N. Engl. J. Med.* **344**, 710–719.

Gaspar P., Ben Jelloun N. and Febvret A. (1994) Sparing of the dopaminergic neurons containing calbindin-D28k and of the dopaminergic mesocortical projections in weaver mutant mice. *J. Neurosci.* **61**, 293–305.

Hitoshi S., Seaberg R. M., Koscik C., Alexson T., Kusunoki S., Kanazawa I., Tsuji S. and Kooy D. (2004) Primitive neural stem cells from the mammalian epiblast differentiate to definitive neural stem cells under the control of Notch signaling. *Genes Dev.* **18**, 1806–1811.

Hwang W. S., Ryu Y. J., Park J. H., Park E. S., Lee E. G., Koo J. M., Jeon H. Y., Lee B. C., Kang S. K., Kim S. J *et al.* (2004) Evidence of a pluripotent human embryonic stem cell line derived from a cloned blastocyst. *Science* **303**, 1669–1674.

Jacobson M. (1991) *Developmental Neurobiology.* Plenum Press, New York.

Johe K. K., Hazel T. G., Muller T., Dugich-Djordjevic M. M. and McKay R. D. (1996) Single factors direct the differentiation of stem cells from the fetal and adult nervous system. *Genes Dev.* **10**, 3129–3140.

Kawasaki H., Mizuseki K., Nishikawa S., Kaneko S., Kuwana Y., Nakanishi S., Nishikawa S.-I. and Sasai Y. (2000) Induction of midbrain dopaminergic neurons from ES cells by stromal cell–derived inducing activity. *Neuron* **28**, 31–40.

Kawasaki H., Suemori H., Mizuseki K., Watanabe K., Urano F., Ichinose H., Haruta M., Takahashi M., Yoshikawa K., Nishikawa S *et al.* (2002) Generation of dopaminergic neurons and pigmented epithelia from primate ES cells by stromal cell-derived inducing activity. *Proc. Natl. Acad. Sci. USA* **99**, 1580–1585.

Kenney A. M. and Rowitch D. H. (2000) Sonic hedgehog promotes G (1) cyclin expression and sustained cell cycle progression in mammalian neuronal precursors. *Mol. Cell. Biol.* **20**, 9055–9067.

Kim J. H., Auerbach J. M., Rodreguez-Gomez J. A., Velasco I., Gavin D., Lumelsky N., Lee S. H., Nguyen J., Sanchez-Pernaute R., Bankiewicz K. and McKay R. D. (2002) Dopamine neurons derived from embryonic stem cells function in an animal model of Parkinson's disease. *Nature* **418**, 50–56.

Kim J. Y., Koh H. C., Lee J. Y., Chang M. Y., Kim Y. C., Chung H. Y., Son H., Lee Y. S., Studer L., McKay R. and Lee S. H. (2003) Dopaminergic neuronal differentiation from rat embryonic neural precursors by Nurr1 overexpression. *J. Neurochem.* **85**, 1443–1454.

Lai K., Kaspar B. K., Gage F. H. and Schaffer D. V. (2003) Sonic hedgehog regulates adult neural progenitor proliferation *in vitro* and *in vivo*. *Nature Neurosci.* **6**, 21–27.

Larsson L. C., Czech K. A., Brundin P. and Widner H. (2000) Intrastriatal ventral mesencephalic xenografts of porcine tissue in rats: immune responses and functional effects. *Cell Transplant.* **9**, 261–272.

Le W., Conneely O. M., He Y., Jankovic J. and Appel S. H. (1999) Reduced Nurr1 expression increases the vulnerability of mesencephalic dopamine neurons to MPTP-induced injury. *J. Neurochem.* **73**, 2218–2221.

Lee S. H., Lumelsky N., Studer L., Auerbach J. and McKay R. D. (2000a) Efficient generation of midbrain and hindbrain neurons from mouse embryonic stem cells. *Nature Biotech.* **18**, 675–679.

Lee S. H., Chang M. Y., Lee K. H., Park B. S., Lee Y. S., Chin H. R. and Lee Y. S. (2000b) Importance of valine at position 152 for the substrate transport and 2 beta-carbomethoxy-3beta-(4-fluorophenyl) tropane binding of dopamine transporter. *Mol. Pharmacol.* **57**, 883–889.

Machold R., Hayashi S., Rutlin M., Muzumdar M. D., Nery S., Corbin J. G., Gritli-Linde A., Dellovade T., Porter J. A., Rubin L. L *et al.* (2003) Sonic hedgehog is required for progenitor cell maintenance in telencephalic stem cell niches. *Neuron* **39**, 937–950.

Okabe S., Forsberg-Nilsson K., Spiro A. C., Segal M. and McKay R. D. (1996) Development of neuronal precursor cells and functional postmitotic neurons from embryonic stem cells in vitro. *Mech. Dev.* **59**, 89–102.

Olsson M., Nikkhah G., Bentlage C. and Borklund A. (1995) Forelimb akinesia in the rat Parkinson model: differential effects of dopamine agonists and nigral transplants as assessed by a new stepping test. *J. Neurosci.* **15**, 3863–3875.

Park J. H., Kim S. J., Oh E. J., Moon S. Y., Roh S. I., Kim C. G. and Yoon H. S. (2003) Establishment and maintenance of human embryonic stem cells on STO, a permanently growing cell line. *Biol. Reprod.* **69**, 2007–2014.

Paxinos G. and Watson C. (1982) *The rat brain in stereotaxic co-ordinates*. Academic Press, San Diego.

Perlmann T. and Wallen-Mackenzie A. (2004) Nurr1, an orphan nuclear receptor with essential functions in developing dopamine cells. *Cell Tissue Res.* **318**, 45–52.

Perrier A. L., Tabar V., Barberi T., Rubio M. E., Bruses J., Topf N., Harrison N. L. and Studer L. (2004) Derivation of midbrain dopamine neurons from human embryonic stem cells. *Proc. Natl. Acad. Sci. USA* **101**, 12 543–12 548.

Piccini P., Brooks D. J., Bjorklund A., Gunn R. N., Grasby P. M., Rimoldi O., Brundin P., Hagell P., Rehncrona S., Widner H. and Lindvall O. (1999) Dopamine release from nigral transplants visualized *in vivo* in a Parkinson's patient. *Nature Neurosci.* **2**, 1137–1140.

Qian X., Shen Q., Goderie S. K., He W., Capela A., Davis A. A. and Temple A. (2000) Timing of CNS cell generation: a programmed sequence of neuron and glial cell production from isolated murine cortical stem cells. *Neuron* **28**, 69–80.

Reubinoff B. E., Pera M. F., Fong C.-Y., Trounson A. and Bongso A. (2000) Embryonic stem cell lines from human blastocysts: somatic differentiation in vitro. *Nature Biotechn* **18**, 399–404.

Rosenblad C., Martinez-Serrano A. and Bjorklund A. (1996) Glial cell line-derived neurotrophic factor increases survival, growth and function of intrastriatal fetal nigral dopaminergic grafts. *Neuroscience* **75**, 979–985.

Shim J. W., Koh H. C., Chang M. Y., Roh E., Choi C. Y., Oh Y. J., Son H., Lee Y. S., Studer L. and Lee S. H. (2004) Enhanced *in vitro* midbrain dopamine neuron differentiation, dopaminergic function, neurite outgrowth, and 1-methyl-4-phenylpyridium resistance in mouse embryonic stem cells overexpressing Bcl-XL. *J. Neurosci.* **24**, 843–852.

Simon H. H., Saueressig H., Wurst W., Goulding M. D. and O'Leary D. D. M. (2001) Fate of Midbrain Dopaminergic Neurons Controlled by the Engrailed Genes. *J. Neurosci.* **21**, 3126–3134.

Smidt M. P., Asbreuk C. H., Cox J. J., Chen H., Johnson R. L. and Burbach J. P. (2000) A second independent pathway for development of mesencephalic dopaminergic neurons requires Lmx1b. *Nature Neurosci.* **3**, 337–341.

Studer L., Tabar V. and McKay R. D. (1998) Transplantation of expanded mesencephalic precursors leads to recovery in parkinsonian rats. *Nature Neurosci.* **1**, 290–295.

Temple S. and Davis A. A. (1994) Isolated rat cortical progenitor cells are maintained in division in vitro by membrane-associated factors. *Development* **120**, 999–1008.

Thibert C., Teillet M. A., Lapointe F., Mazelin L., Le Douarin N. M. and Mehlen P. (2003) Inhibition of neuroepithelial patched-induced apoptosis by sonic hedgehog. *Science* **301**, 843–846.

Yamada T., McGeer P. L., Baimbridge K. G. and McGeer E. G. (1990) Relative sparing in Parkinson's disease of substantia nigra dopamine neurons containing calbindin-D28K. *Brain Res.* **526**, 303–307.

Ye W., Shimamura K., Rubenstein J. L., Hymes M. A. and Rosenthal A. (1998) FGF and Shh signals control dopaminergic and serotonergic cell fate in the anterior neural plate. *Cell* **93**, 755–766.

Zawada W. M., Zastrow D. J., Clarkson E. D., Adams F. S., Bell K. P. and Feed C. R. (1998) Growth factors improve immediate survival of embryonic dopamine neurons after transplantation into rats. *Brain Res.* **786**, 96–103.

Zeng X., Cai J., Chen J., Luo Y., You Z.-B., Fotter E., Wang Y., Harvey B., Miura T., Backman C *et al.* (2004) Dopaminergic differentiation of human embryonic stem cells. *Stem Cells* **22**, 925–940.